



Constraints from uranium and molybdenum isotope ratios on the origin of enriched mid-ocean ridge basalts

Joel B. Rodney^{a,*}, Morten B. Andersen^b, Bramley J. Murton^c, Tim Elliott^a

^a Bristol Isotope Group, School of Earth Sciences, University of Bristol, Wills Memorial Building, Queen's Road, Bristol, BS8 1RJ, UK

^b School of Earth & Environmental Sciences, Cardiff University, Park Place, Cardiff, CF10 3AT, UK

^c National Oceanography Centre, Waterfront Campus, European Way, Southampton, SO14 3ZH, UK

ARTICLE INFO

Editor: Prof. Fang-Zhen Teng

Keywords:

U isotopes
Mo isotopes
Enriched MORB
Crustal recycling
Low degree partial melting

ABSTRACT

Most mid-ocean ridge basalts (MORB) are depleted in highly incompatible elements relative to the primitive mantle and are termed normal (N)-MORB. Some MORB, erupted at ridge segments distal from mantle hot-spots, are enriched in incompatible elements. The origin of these enriched (E)-MORB is debated, although many studies have proposed that recycled oceanic crust shapes their compositions. Uranium (U) and molybdenum (Mo) isotope ratios have been argued to trace the contribution of recycled oceanic crust in the source of N-MORB, which has high $\delta^{238}\text{U}$ and low $\delta^{98/95}\text{Mo}$ relative to the bulk silicate Earth (BSE). Here, we provide U and Mo isotopic data on E-MORB samples from the northern mid-Atlantic ridge (13° & 45° N). We analysed hand-picked, leached MORB glass, yielding $^{234}\text{U}/^{238}\text{U}$ near secular equilibrium, therefore reflecting samples unperturbed by surface processes. Samples have uniform $\delta^{238}\text{U}$ and $\delta^{98/95}\text{Mo}$, with means of -0.307 ± 0.032 ‰, 2sd, and -0.14 ± 0.04 ‰, 2sd, respectively, both within uncertainty of BSE, and distinct from N-MORB. These data, as well as unremarkable Ce/Pb and radiogenic Pb isotopic compositions in E-MORB globally, are incompatible with their sources containing recycled oceanic crust or continental derived sediments. Instead, our data fit with a model of low degree partial melting of the uppermost mantle that metasomatises the sub-oceanic lithosphere. Given BSE-like U isotopic compositions of E-MORB, that are isotopically unfractionated during low degree partial melting, we suggest that the initial melting event must have occurred prior to the recycling of isotopically distinct in U oceanic crust into the upper mantle (i.e., prior to ca. 600 Ma, the estimated time of deep ocean oxygenation). Metasomatised portions of oceanic lithospheric mantle preserve these ≥ 600 Ma U isotopic compositions, which are subducted and stirred back into the convecting upper mantle, ultimately to be sampled at ridges as E-MORB. Molybdenum isotopic compositions of E-MORB are in line with such a model but also reflect isotopic fractionation to higher $\delta^{98/95}\text{Mo}$ during low degree partial melting of ≥ 600 Ma upper mantle, that counter acts the lowering of $\delta^{98/95}\text{Mo}$ in the upper mantle by an on-going process of plate recycling.

1. Introduction

Mid-ocean ridge basalts (MORB), magmatic samples of the upper mantle, are chemically heterogeneous and commonly split into two groups according to their 'incompatible' element compositions (Fig. 1) (e.g., Schilling, 1975; Gale et al., 2013). Along the majority of mid-ocean ridge (MOR) segments, basalts erupted have 'depleted' signatures, with ratios of more to less incompatible elements lower than estimates of the primitive mantle (e.g., La/Sm normalized to primitive mantle, $(\text{La}/\text{Sm})_{\text{N}} < 1$) (Fig. 1) (McDonough and Sun, 1995). Rarer, enriched (E)-MORB have incompatible element abundances markedly higher than N-MORB

and are associated with elevated ratios of more to less incompatible elements (e.g., $(\text{La}/\text{Sm})_{\text{N}} \geq 1$) and distinctive isotopic signatures (e.g., radiogenic $^{87}\text{Sr}/^{86}\text{Sr}$). While their presence is well documented, the exact definition of E-MORB varies in different studies (Fig. 1).

Some E-MORB locations are from topographically elevated MOR sections and are linked to enrichments from hot-spots, upwellings from greater depth (Schilling, 1975; Schilling et al., 1985). However, for E-MORB that occur at MOR segments far from the influence of hot-spots, the origin of the chemical enrichment is debated. It has been proposed that recycling of oceanic crust and/or continental sediments into the upper mantle causes enrichment (e.g., Allègre and Turcotte, 1986;

* Corresponding author.

E-mail addresses: joel.rodney@bristol.ac.uk (J.B. Rodney), andersem1@cardiff.ac.uk (M.B. Andersen), bramley.murton@noc.ac.uk (B.J. Murton), tim.elliott@bristol.ac.uk (T. Elliott).

<https://doi.org/10.1016/j.epsl.2025.119491>

Received 15 November 2024; Received in revised form 30 May 2025; Accepted 3 June 2025

Available online 11 June 2025

0012-821X/© 2025 The Author(s). Published by Elsevier B.V. This is an open access article under the CC BY license (<http://creativecommons.org/licenses/by/4.0/>).

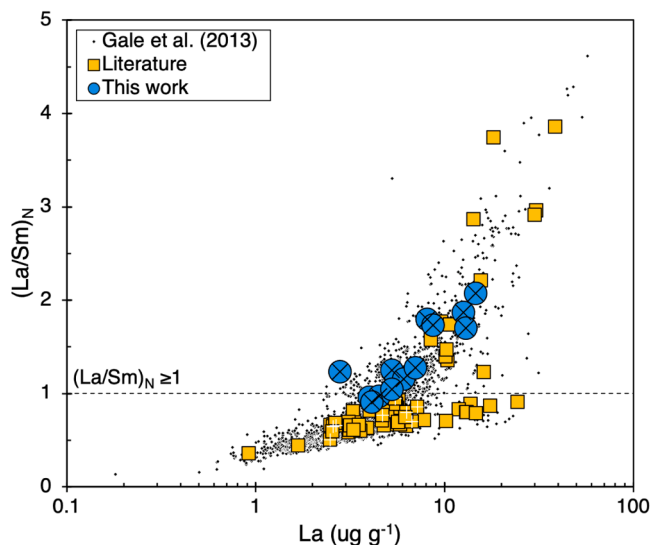


Fig. 1. Global MORB variations in chemical enrichment based on $(\text{La}/\text{Sm})_N$. Mid-ocean ridge basalts database from Gale et al. (2013) shown as small black diamonds. Literature MORB data with Mo and/or U isotopic data are shown as yellow squares (Andersen et al., 2015; Bezzard et al., 2016; Chen et al., 2022; Hin et al., 2022). Mid-ocean ridge basalt samples analysed in this study are shown as larger blue circles. Samples in this work and literature data with both Mo and U isotope data are shown with black crosses (E-MORB) or white plus signs (N-MORB).

Prinzhofer et al., 1989; Hémond et al., 2006; Waters et al., 2011; Ulrich et al., 2012; Yang et al., 2020), similar to models of source enrichment in ocean island basalts (OIB). Other works argue for low degree partial melting and two stage melting models, either with or without recycled crustal material. Donnelly et al. (2004) argue for low degree partial melting of subducting crust that enriches the convecting mantle wedge at subduction zones. This enriched mantle is stirred into the wider upper mantle and can be sampled at ridges giving rise to E-MORB. Nielsen et al., (2018) propose a similar model but also argue for the addition of subducted sediment to the overlying mantle that induces low degree partial melting to produce the E-MORB reservoir that is ultimately sampled under ridges. Scenarios that do not invoke recycled crustal material in the E-MORB source argue for low degree partial melts of the uppermost mantle that metasomatise oceanic mantle lithosphere, enriching portions of mantle that are subsequently subducted back into the upper mantle and sampled at ridges (e.g., Green, 1971; Kostopoulos and Murton, 1992; Halliday et al., 1995; Niu et al., 2002; Chen et al., 2022; Guo et al., 2023).

Measurements of novel stable isotope ratios can be used to investigate upper mantle chemical heterogeneity and enrichment. Uranium (U) and molybdenum (Mo) are useful for tracing processes of crustal recycling due to large low temperature isotopic fractionations that occur during seafloor alteration of the oceanic crust, sediment deposition (Andersen et al., 2015; Freymuth et al., 2015; Ahmad et al., 2021), and during the dehydration of subducting slabs in subduction zones (Andersen et al., 2015; Freymuth et al., 2015, 2019; König et al., 2016; Gaschnig et al., 2017; Villalobos-Orchard et al., 2020; Ahmad et al., 2021). Here we express Mo isotope ratios as $\delta^{98/95}\text{Mo}_{\text{NIST SRM3134}}$ (the relative difference in $^{98}\text{Mo}/^{95}\text{Mo}$ between samples and standard reference material NIST SRM3134, hereafter written $\delta^{98/95}\text{Mo}$ in the text), and U isotope ratios as $\delta^{238}\text{U}_{\text{CRM145}}$ (the relative difference in $^{238}\text{U}/^{235}\text{U}$ between samples and certified reference material CRM-145, hereafter written $\delta^{238}\text{U}$ in the text).

Slab dehydration during subduction releases oxidising fluids with high $\delta^{98/95}\text{Mo}$ and low $\delta^{238}\text{U}$ into the overlying mantle wedge, as inferred from the compositions of volcanic arc lavas (Andersen et al., 2015; Freymuth et al., 2015, 2019; König et al., 2016; Gaschnig et al.,

2017; Villalobos-Orchard et al., 2020) (Fig. 2). Exhumed eclogites and metasediments with low $\delta^{98/95}\text{Mo}$ also reflect this process (Fig. 2a) (Chen et al., 2019; Ahmad et al., 2021). Additionally, in some cases mafic oceanic crust has acquired a low $\delta^{98/95}\text{Mo}$ through seafloor alteration before subduction zone processing (Ahmad et al., 2021). The U isotopic system further reflects the importance of seawater alteration of the oceanic crust (Fig. 2b). Seawater alteration of oceanic crust greatly increases its U concentration (e.g., Staudigel et al., 1995) with the added U, on average, being isotopically heavy (Andersen et al., 2015, 2024). Subducting slab dehydration and seawater alteration therefore result in residual slabs with compositions that are isotopically light in Mo and isotopically heavy in U. The recycling of Mo and U from this crustal material into the upper mantle is inferred from compositions of N-MORB samples that are isotopically lighter in Mo and heavier in U than the bulk silicate Earth (BSE) as defined by chondrites (Burkhardt et al., 2014; Andersen et al., 2015; Hin et al., 2022) (Fig. 2). This can also be seen in higher Ce/Mo ratios and lower Th/U ratios of N-MORB than the BSE. Cerium and Th are of similar incompatibility to Mo and U respectively during mantle melting, but with different fluid mobility; Mo and U are aqueous fluid mobile, Ce and Th are not.

Following the onset of the first major rise in atmospheric oxygen (~ 2.3 Ga), there would have been a supply of continental derived U to the oceans due to oxidative weathering. The recycling of oceanic crust with excess U relative to immobile Th has been used to explain the lower measured $^{232}\text{Th}/^{238}\text{U}$ in MORB relative to the time integrated $^{232}\text{Th}/^{238}\text{U}$ ratio calculated from Pb isotopic compositions (e.g., Zartman and Haines, 1988; McCulloch, 1993; Collerson and Kamber, 1999; Elliott et al., 1999). Isotopically perturbed U, however, may only have been recycled into the mantle since the Neoproterozoic oxygenation event, ~ 600 Ma (e.g., Lyons et al., 2014), given that imparting high $\delta^{238}\text{U}$ to altered oceanic crust (AOC) requires oxygenated deep oceans (Andersen et al., 2015, 2024). Isotopically perturbed Mo, in contrast, has potentially been recycled into the N-MORB source since the onset of modern day like plate tectonics and mass balance models suggest that at least ~ 1 Gyr of crustal recycling is needed to cause the observed shift in N-MORB $\delta^{98/95}\text{Mo}$ from BSE compositions (Hin et al., 2022).

Molybdenum and U isotopes offer a way to investigate if recycled oceanic crust is mixed into the E-MORB source and provide constraints on the timescales it takes to 'pollute' the upper mantle with surface derived material. Recent studies have shown some E-MORB have chondritic or slightly higher values of $\delta^{98/95}\text{Mo}$ and are resolvable from N-MORB (Bezzard et al., 2016; Chen et al., 2022). To assess if this is a ubiquitous feature, there is need for data from different geographic regions, as well as for measurements of both $\delta^{98/95}\text{Mo}$ and $\delta^{238}\text{U}$ on the same samples. Herein we combine Mo with U isotopic measurements on a set of E-MORB samples from the northern Mid-Atlantic ridge (MAR) as a diagnostic test for recycled crustal components in the E-MORB source.

2. Geological location and samples

We report U and Mo elemental and isotopic compositions for sixteen MAR E-MORB samples, located at $\sim 13^\circ \text{N } 44^\circ \text{W}$ (five samples) and $45^\circ \text{N } 28^\circ \text{W}$ (eleven samples) that span MgO contents from ~ 10 to 7 wt. %. Our samples are chemically enriched, with either $(\text{La}/\text{Sm})_N \geq 1$ and or $\text{K}_2\text{O}/\text{TiO}_2 \geq 0.11$. Enriched-MORB in the $13^\circ \text{N } 44^\circ \text{W}$ segment are common, and basalts have up to forty times higher concentrations of highly incompatible elements than N-MORB from segments nearby (Bougault et al., 1988). Samples from $13^\circ \text{N } 44^\circ \text{W}$ were collected by dredging in the RSS James Cook JC007 cruise in March – April 2007 (Wilson et al., 2013) (Table S1). They represent a group of basalts erupted before the formation of oceanic core complexes in the area, and now sit off-axis, having been erupted at $\sim 0.5 - 1$ Ma. Samples from $\sim 45^\circ \text{N } 28^\circ \text{W}$ are also from a region where E-MORB commonly occurs (Bougault et al., 1988) and samples were collected *in situ* during RSS James Cook cruise JC024 May – June 2008 and are all < 3 Ma (Table S1) (Searle et al., 2010). Major and trace element data for both sample sets

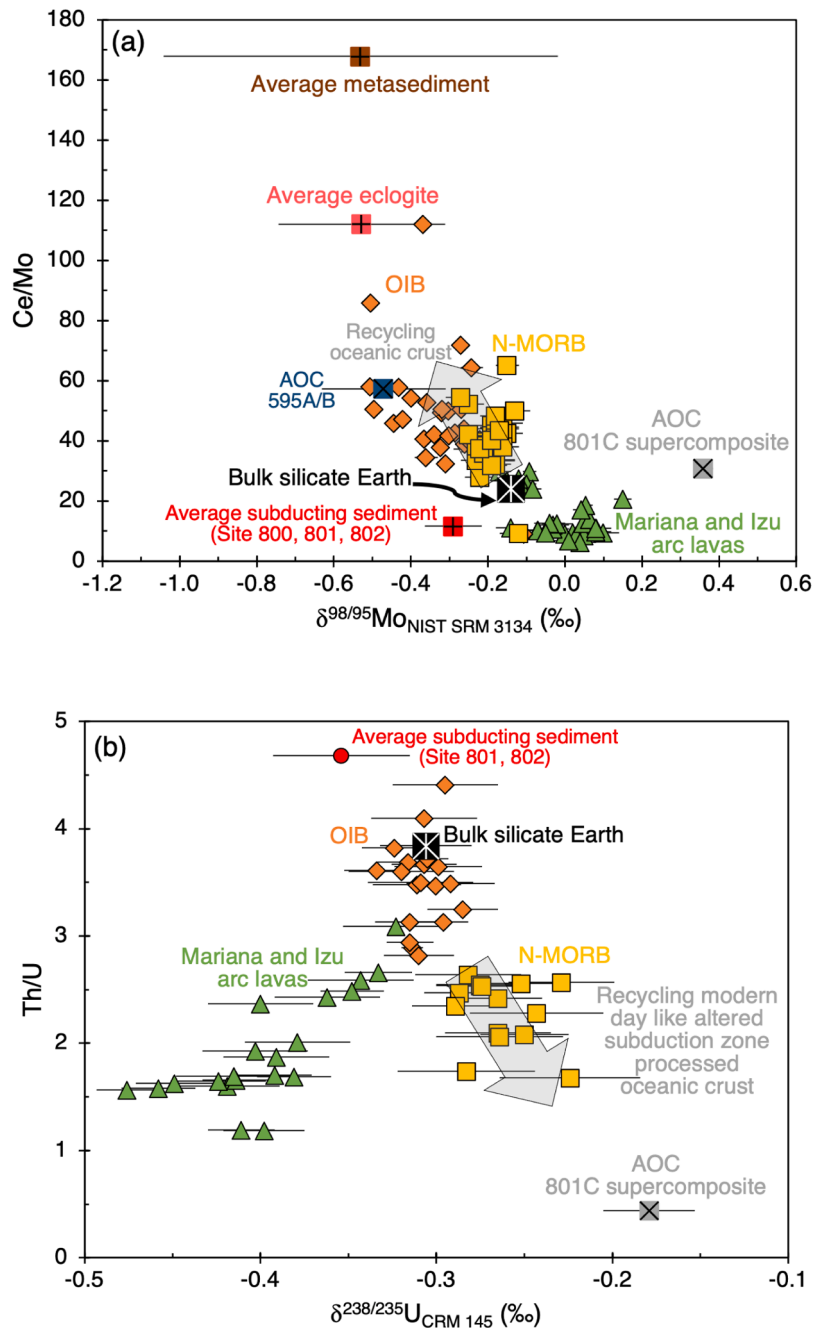


Fig. 2. (a) $\delta^{98/95}\text{Mo}$ versus Ce/Mo and (b) $\delta^{238/235}\text{U}$ versus Th/U for mantle derived basalts, AOC, subduction processed N-MORB-like eclogite and subducting sediment. Ocean island basalts (orange diamonds) are from Willbold and Elliott (2023) and Andersen et al. (2015). Volcanic arc lavas from the Mariana and Izu arc (green triangles) are from Freymuth et al. (2015, 2019), Andersen et al. (2015), and Villalobos-Orchard et al. (2020). Bulk silicate Earth compositions (black starred square) are from Hin et al. (2022) and Andersen et al. (2015). Average Western Pacific subducting sediment composition (red square with a plus sign) is from Ocean Drilling Programme sites 800, 801, and 802 from Andersen et al. (2015) and Freymuth et al. (2015). We use the global average subducting sediment Th/U ratio from Plank (2014) GLOSS-II. Average compositions of AOC from the 801C supercomposite (grey crossed square) are from Andersen et al. (2015) and Freymuth et al. (2015). Average AOC from 595A/B (blue crossed square) is the average composition, $\pm 1\text{sd}$, weighted by Mo concentration from Ahmad et al. (2021). Average composition, $\pm 1\text{sd}$, weighted by Mo concentration of a set of exhumed eclogites (pink square with a plus sign) are from Chen et al. (2019) and Ahmad et al. (2021). Average composition, $\pm 1\text{sd}$, weighted by Mo concentration of metasediments (brown square with a plus sign) is from Ahmad et al. (2021). Mid-ocean ridge basalt data (yellow squares) are from Andersen et al. (2015), Bezard et al. (2016), Chen et al. (2022), and Hin et al. (2022). For MORB Mo data we follow the filtering of Hin et al. (2022), where two anomalous samples from Bezard et al. (2016) are excluded, as they do so themselves. We also exclude all data from Liang et al. (2017), whose data cannot be reproduced and show markedly higher $\delta^{98/95}\text{Mo}$ compositions for MORB samples than Bezard et al. (2016) and Chen et al. (2022), see Hin et al. (2022) for details. Grey arrows show the effect of mixing recycled oceanic crust into the mantle.

were collected following the methods in Wilson et al. (2013).

The Azores hot-spot at $\sim 38^\circ\text{N } 28^\circ\text{W}$, which forms the Azores Island chain sitting to the east of the MAR, is the closest mantle hot-spot to both sample sites. The Azores hot-spot interacts with the MAR, causing

nearby ridge segments to become broader and shallower. Material from the Azores hot-spot flows southwards along the ridge, with elevated La/Sm ratios between 35° to 40°N . More N-MORB like compositions occur below 30°N and above 40°N , with no detectable effects of the hot-spot

further south than 26° N (e.g., [Maia et al., 2007](#)). Our sample sites sit outside the zone of influence of the Azores hot-spot, and geochemical enrichment is not linked to hot-spot-ridge interaction ([Bougault et al., 1988](#)).

3. Methods

Fresh MORB glass was crushed and processed to ~ 600 µm size chips, using an agate pestle and mortar. To avoid samples potentially affected by seawater alteration (e.g., Fe-Mn oxide coatings), samples were hand-picked under a binocular microscope to ensure samples were optically clear and devoid of potential alteration. While this process has long been employed, notably in U-series disequilibrium studies (e.g., [Reinitz and Turekian, 1989](#)), it is laborious, and considering the quantities needed for isotopic analysis (e.g., >1 g), it is a rate limiting step. Hand picking MORB glass is also subjective, and it is unclear what defines an acceptable limit of quality. A reliable check of sample alteration in young samples is given by measurements of $^{234}\text{U}/^{238}\text{U}$ activity ratios. If unaffected by recent seawater alteration, the ^{238}U decay chain will be in secular equilibrium, and so the activity ratio of $^{234}\text{U}/^{238}\text{U}$, typically expressed as ($^{234}\text{U}/^{238}\text{U}$), will be unity. Seawater has ($^{234}\text{U}/^{238}\text{U}$) ~ 1.14 (e.g., [Kipp et al., 2022](#)) and elevated ($^{234}\text{U}/^{238}\text{U}$) in samples may indicate the addition of seawater U and other elements onto Fe-Mn oxide coatings ([Siebert et al., 2003](#); [Hin et al., 2022](#)). We explored variously stringent picking strategies on samples and up to three different splits of glass of varying quality (A, B, and C in decreasing order of quality) were prepared (classifications are detailed in Supplementary Material: [Section 1](#)) (Fig. S1). In some cases, different splits were combined to ensure there was enough sample to measure.

Samples also underwent a reductive leaching step (Supplementary Material: [Section 1](#)) prior to dissolution to remove secondary coatings. Samples were leached with a mixture of 0.05 M hydroxylamine hydrochloride, 15 % acetic acid and 0.03 M Na-EDTA buffered to pH 4 with NaOH ([Gutjahr et al., 2007](#)). [Andersen et al. \(2015\)](#) and [Hin et al. \(2022\)](#) note that leaching can result in some glass dissolution, and minor U and Mo loss (Fig. S2). Ratios of the concentrations of elements that absorb to Fe-Mn coatings such as U and Mo to those little affected, such as Th, that would only be removed during glass dissolution, were monitored to examine the effects of leaching. Samples of JC24-82-21 were prepared and analysed before other samples to calibrate methods. This sample was leached three times and results indicated that one to two leaching steps were sufficient to remove any apparent chemical signature of Fe-Mn coatings (Fig. S3). For other samples we opted for two leaching steps, although note that one step is likely sufficient.

Uranium isotopic measurement methods followed [Andersen et al. \(2015\)](#), and Mo isotopic measurement methods followed [Willbold et al. \(2016\)](#) and [Hin et al. \(2022\)](#), as detailed fully in Supplementary Material: [Section 2](#). Uranium and Mo isotope analyses were conducted in the Bristol Isotope Group labs, University of Bristol. Approximately 0.5 to 1 g of MORB glass was dissolved and after achieving full dissolution, a ~ 1 % fraction of samples was measured on an Element2 ICP-MS for Th, U, and Mo concentration ([Andersen et al., 2014](#)). Measured reference materials are in good agreement with literature values (Supplementary Material: [Section 2](#)) (Table S2).

Samples were spiked with the IRMM3636 $^{236}\text{U} - ^{233}\text{U}$ 50:50 double spike ([Richter et al., 2008](#)) aiming for a $^{236}\text{U}/^{235}\text{U}$ ratio of 5. Samples were also spiked with an in-house $^{97}\text{Mo} - ^{100}\text{Mo}$ double spike, with a $^{97}\text{Mo}/^{95}\text{Mo}$ ratio of 47.58 and $^{100}\text{Mo}/^{95}\text{Mo}$ ratio of 58.32, aiming for a natural Mo-double spike Mo proportion of 0.5.

Purification and U separation used a two-column method, with TRU resin to separate most matrix elements, including all Mo, followed by UTEVA resin to separate Th from U. An aliquot containing Mo from the first separation column was collected for later processing. Final U aliquots were dissolved in 0.2 M HCl (aiming for U concentration of 100 – 300 ng g⁻¹) for isotopic analysis. Procedural blanks were <30 pg U, negligible compared to amount of U consumed per measurement, 30 –

80 ng.

Uranium isotope compositions were measured on a ThermoFinnigan Neptune MC-ICP-MS (serial no. 1002) in low mass resolution ($M/\Delta M \sim 2000$, 5 to 95 % peak height definition). Samples were introduced into the plasma using a ~ 40 ul min⁻¹ micro-concentric PFA nebuliser connected to a Cetac Aridus (1st generation) desolvating system. Masses 232 (^{232}Th), 233 (^{233}U), 234 (^{234}U), 235 (^{235}U), 236 (^{236}U), and 238 (^{238}U) were measured simultaneously. Each sample was preceded and followed by a measurement of the double-spiked CRM-145 standard. Individual measurements consisted of 80 cycles, with 4.194 s integration time.

Uranium isotope ratios for $^{238}\text{U}/^{235}\text{U}$ and $^{234}\text{U}/^{238}\text{U}$ were calculated using the exponential mass fractionation law and double spike $^{233}\text{U}/^{236}\text{U}$ ratio ([Richter et al., 2008](#)). Data reported are normalised to the average of the bracketing CRM-145 standard, with $^{234}\text{U}/^{238}\text{U}$ ratios reported in delta notation relative to secular equilibrium where secular equilibrium is 0 and CRM-145 has a $\delta^{234}\text{U}$ value of -38.6 ‰ ([Cheng et al., 2013](#)).

External reproducibility of all samples has been determined from the long-term external reproducibility of BHVO-2 measured at various intensities (Supplementary Material: [Section 2](#)). This results in an estimated external reproducibility of $\delta^{238}\text{U}$ and $\delta^{234}\text{U}$ from ± 0.09 to 0.03 ‰, 2sd, and ± 4 to 0.9 ‰, 2sd, for ^{238}U intensities from 200 – 1000 pA ranges respectively (Fig. S4). Uranium isotopic measurements of international reference materials (BHVO-2, BCR-2, BIR, W-2A, and CZ-1) agree with literature values (Table S3).

Collected Mo fractions from the TRU resin U chemistry were dried and dissolved for Mo chemistry using Eichrom AG 1-X8 anionic resin. Final Mo collections were dried and re-dissolved in 0.4 M HNO₃ – 0.4 M HF for a Mo concentration of 200 ng g⁻¹ for isotopic analysis. Procedural blanks were <400 pg Mo, negligible compared to the amount of Mo consumed per measurement, ~ 30 ng.

Molybdenum isotope compositions were measured on a ThermoFinnigan Neptune MC-ICP-MS (serial no. 1020) in low mass resolution ($M/\Delta M \sim 1600$, 5 to 95 % peak height definition). Samples were introduced to the plasma using a ~ 40 ul min⁻¹ micro-concentric PFA nebuliser connected to a Cetac Aridus (1st generation) desolvating system. Masses 91 (^{91}Zr), 92 (^{92}Mo), 95 (^{95}Mo), 96 (^{96}Mo), 97 (^{97}Mo), 98 (^{98}Mo), 99 (^{99}Ru), 100 (^{100}Mo), and 101 (^{101}Ru) were measured simultaneously. Each sample was preceded and followed by a measurement of the double-spiked standard NIST SRM3134. Individual measurements consisted of 30 cycles, with 4.194 s integration time.

Measurements were internally normalised with a double spike inversion using the isotopes ^{95}Mo , ^{97}Mo , ^{98}Mo , and ^{100}Mo . Samples were then externally normalised to the spiked bracketing standard NIST SRM3134 to calculate $\delta^{98/95}\text{Mo}$. Data were corrected for ^{98}Ru and ^{100}Ru interferences using both ^{99}Ru and ^{101}Ru respectively as monitors of Ru intensity; both corrections yielded the same Mo isotope ratios within uncertainty of one another and uncorrected data. We take a homoscedastic approach to determine our external reproducibility, pooled 2sd, on any single stable Mo isotopic measurement (i.e., one standard-sample-standard measurement) (Table S4). Using this approach, we define an external reproducibility of $\delta^{98/95}\text{Mo} \pm 0.05$ ‰, 2sd, for a single measurement in a given run. This pooled 2sd is then used to calculate the standard error for a given sample given the number, n, of repeat measurements, typically 4 to 6 for unknown samples. This is identical to the 2sd, ± 0.05 ‰, of 35 repeats of W-2A measured over 4 digestions across 4 measuring sessions, and is similar to that reported in [Chen et al. \(2022\)](#) and [Hin et al. \(2022\)](#). Molybdenum isotopic measurements of international reference materials (BHVO-2, BCR-2, and W-2A) agree with literature data (Table S5).

4. Results

Our MAR samples have chemical enrichments from (La/Sm)_N 0.91 to 2.07 (K₂O/TiO₂ 0.11 to 0.37) (Fig. 1, table S6). Uranium concentrations range from 101 to 443 ng g⁻¹, all enriched relative to average N-MORB

(83 ng g⁻¹, Gale et al., 2013) (Table S6). Molybdenum concentrations range from 189 to 967 ng g⁻¹, which is above and below average N-MORB (360 ng g⁻¹, Gale et al., 2013) (Table S6). There are positive correlations between U and Mo concentrations with (La/Sm)_N (Fig. 3a, b).

Values of δ²³⁸U show little variation between -0.331 ± 0.019 ‰, 2se, and -0.263 ± 0.028 ‰, 2se, with a concentration weighted average of -0.307 ± 0.032 ‰, 2sd, (Fig. 3c, table S6). The variability is similar to our long-term external reproducibility of samples measured at similar conditions ~ ± 0.03 ‰ and reflects a near uniform composition of our sample set. The δ²³⁸U compositions of the different qualities of glass picked and leached are all, bar one sample, within analytical uncertainty (Fig. S5a). Also, samples, bar JC24-89-13, are within uncertainty of secular equilibrium (Fig. S5b). Sample JC24-89-13, which is only +2.5 ‰ in δ²³⁴U (Fig. S5b), also has a similar δ²³⁸U to other samples (Fig. S5a). Our E-MORB δ²³⁸U average is lower than global N-MORB, which has a concentration weighted average of -0.259 ± 0.041 ‰, 2sd, (Andersen et al., 2015) (Fig. 3c). We also report δ²³⁸U data for four N-MORB samples from the Indian ocean basin (04/13C, 05/15G, 08/26F, 12/37F) additional to the N-MORB samples in Andersen et al. (2015), but reported in Hin et al. (2022) for ²³⁴U/²³⁸U data. These data are provided in the supplementary material and were collected following methods in Andersen et al. (2015). Our E-MORB δ²³⁸U average is indistinguishable from BSE, δ²³⁸U -0.306 ± 0.026 ‰, 2se, (Andersen et al., 2015).

Molybdenum isotopic compositions show little variation with δ⁹⁸/⁹⁵Mo ranging between -0.11 ± 0.01 ‰, 2se, and -0.19 ± 0.02 ‰, 2se, and are within analytical uncertainty of a concentration weighted average of -0.14 ± 0.04 ‰, 2sd, (Fig. 3d, table S6). The variability, ±0.04 ‰, 2sd, is smaller than our long-term external reproducibility and reflects the near uniform composition of our sample set. Our E-MORB concentration weighted average δ⁹⁸/⁹⁵Mo is indistinguishable from the

value reported in Hin et al., (2022) for global E-MORB, -0.12 ± 0.03 ‰, 95 % c.i. The δ⁹⁸/⁹⁵Mo compositions of the different qualities of glass picked and leached are all within analytical uncertainty (Fig. S5c). Our E-MORB δ⁹⁸/⁹⁵Mo average is higher than global N-MORB, δ⁹⁸/⁹⁵Mo -0.19 ± 0.01 ‰, 95 % c.i. and indistinguishable from BSE, δ⁹⁸/⁹⁵Mo -0.14 ± 0.02 ‰, 95 % c.i. (Fig. 3d) (Hin et al., 2022).

There are no correlations of δ²³⁸U and δ⁹⁸/⁹⁵Mo in our E-MORB samples with tracers of chemical enrichment (Fig. 3c, d) or magmatic differentiation (Fig. S6). Samples from 13° N and 45° N show no resolvable differences and we find no reason to treat each site differently. In summary, the concentration weighted averages of δ²³⁸U and δ⁹⁸/⁹⁵Mo for our E-MORB samples is distinct from global N-MORB, but indistinguishable from BSE (Fig. 3c, d) (Andersen et al., 2015; Hin et al., 2022).

5. Discussion

5.1. Potential alteration of U and Mo isotopes

The reductive leaching process removed some U but little Mo, reflecting the presence of minimal secondary mineral hosted Mo (Supplementary Material: Section 1) (Fig. S2). The different qualities of picked glass for each sample measured showed similar patterns in leaching and are all largely within uncertainty in δ²³⁸U, δ⁹⁸/⁹⁵Mo, and δ²³⁴U (all near secular equilibrium) (Fig. S3, S5). We therefore average all different splits measured for samples into overall δ²³⁸U, δ⁹⁸/⁹⁵Mo, and δ²³⁴U compositions for each sample (Supplementary material: section 1). We further test that our hand-picked MORB glass samples reflect primary magmatic compositions by examining mixing relationships between our average E-MORB compositions and predicted compositions of Fe-Mn crusts. Iron-Mn crusts acquire U from seawater, with elevated δ²³⁴U, and have low δ²³⁸U and δ⁹⁸/⁹⁵Mo, ~ -0.69 ‰ and -0.92 ‰

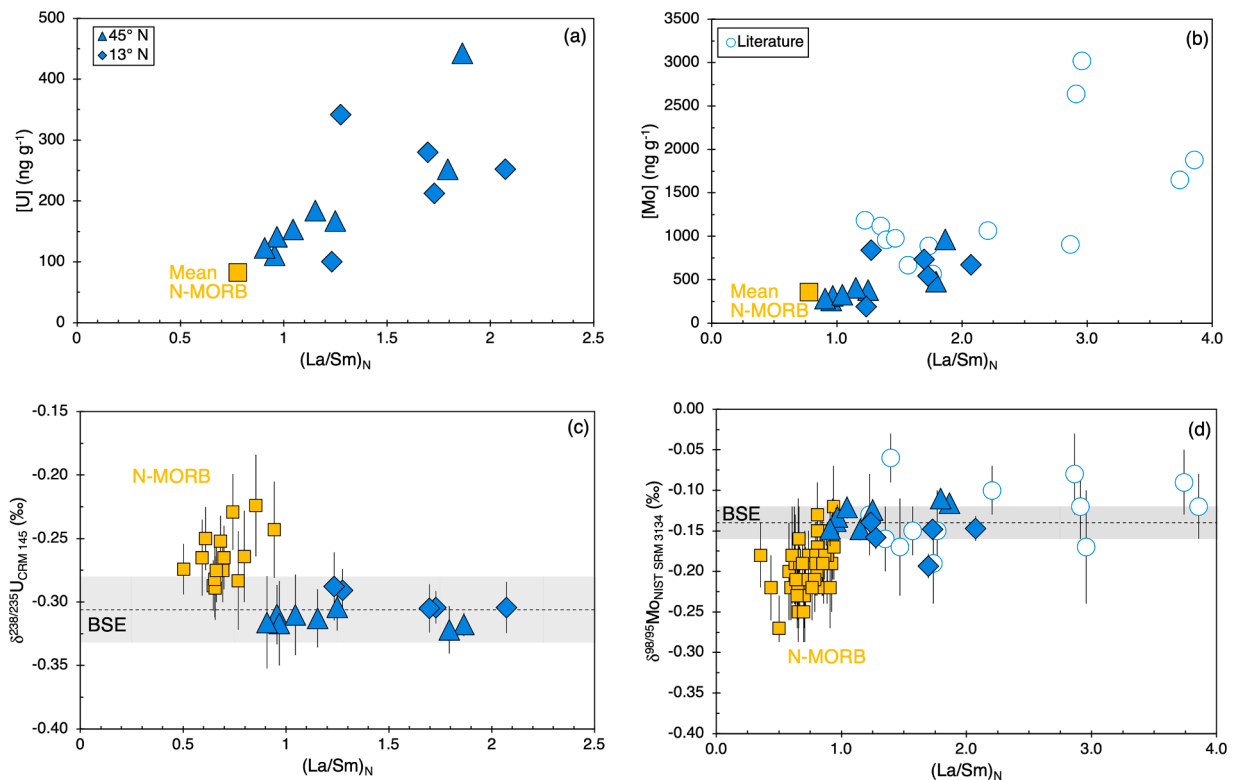


Fig. 3. (a) U and (b) Mo concentrations and (c) δ²³⁸U and (d) δ⁹⁸/⁹⁵Mo versus (La/Sm)_N of MORB samples. Enriched-MORB from this study are shown as filled blue symbols and grouped into samples from 45° N (triangles) and 13° N (diamonds) and shown with ± 2se uncertainties. Average N-MORB (yellow squares) concentrations are from Gale et al. (2013). Isotopic data for BSE and N-MORB are from the same sources as in figure 2, and literature E-MORB (hollow circles) are from Bezard et al. (2016), Chen et al. (2022) and Hin et al. (2022). Grey shaded regions represents isotopic compositions of BSE (± 2se).

respectively (Siebert et al., 2003; Goto et al., 2014). In a binary mixing calculation between our average E-MORB composition and Fe-Mn crusts in $\delta^{238}\text{U}$ - $\delta^{234}\text{U}$ and $\delta^{98/95}\text{Mo}$ - $\delta^{234}\text{U}$ space, our samples do not form arrays towards the composition of Fe-Mn crusts (Fig. 4). The minor variability in $\delta^{238}\text{U}$ and $\delta^{98/95}\text{Mo}$ appears unrelated to $\delta^{234}\text{U}$, and the samples with minor deviations in $\delta^{234}\text{U}$ from secular equilibrium do not show compositions systematically perturbed towards Fe-Mn crusts in either U or Mo isotopic compositions (Fig. 4). We therefore infer that the $\delta^{238}\text{U}$ and $\delta^{98/95}\text{Mo}$ of the samples represent primary values.

5.2. Fractional crystallisation

Our data spans a narrow range of MgO content (10.2 to 6.9 wt. %) and show no correlation in $\delta^{98/95}\text{Mo}$ and $\delta^{238}\text{U}$ with magmatic differentiation (Fig. S6). This is in accordance with other studies that show no resolvable correlation of $\delta^{98/95}\text{Mo}$ in MORB with MgO over a wider range of compositions, 1.8 to 9.5 wt.% (Bezard et al., 2016; Chen et al., 2022). Our samples also reflect the similar incompatibilities of U & Th and Mo & Ce during magmatic differentiation (Fig. S6), with near constant ratios of ~ 3 and ~ 35 respectively, in keeping with wider data for seafloor basalts (e.g., Gale et al., 2013).

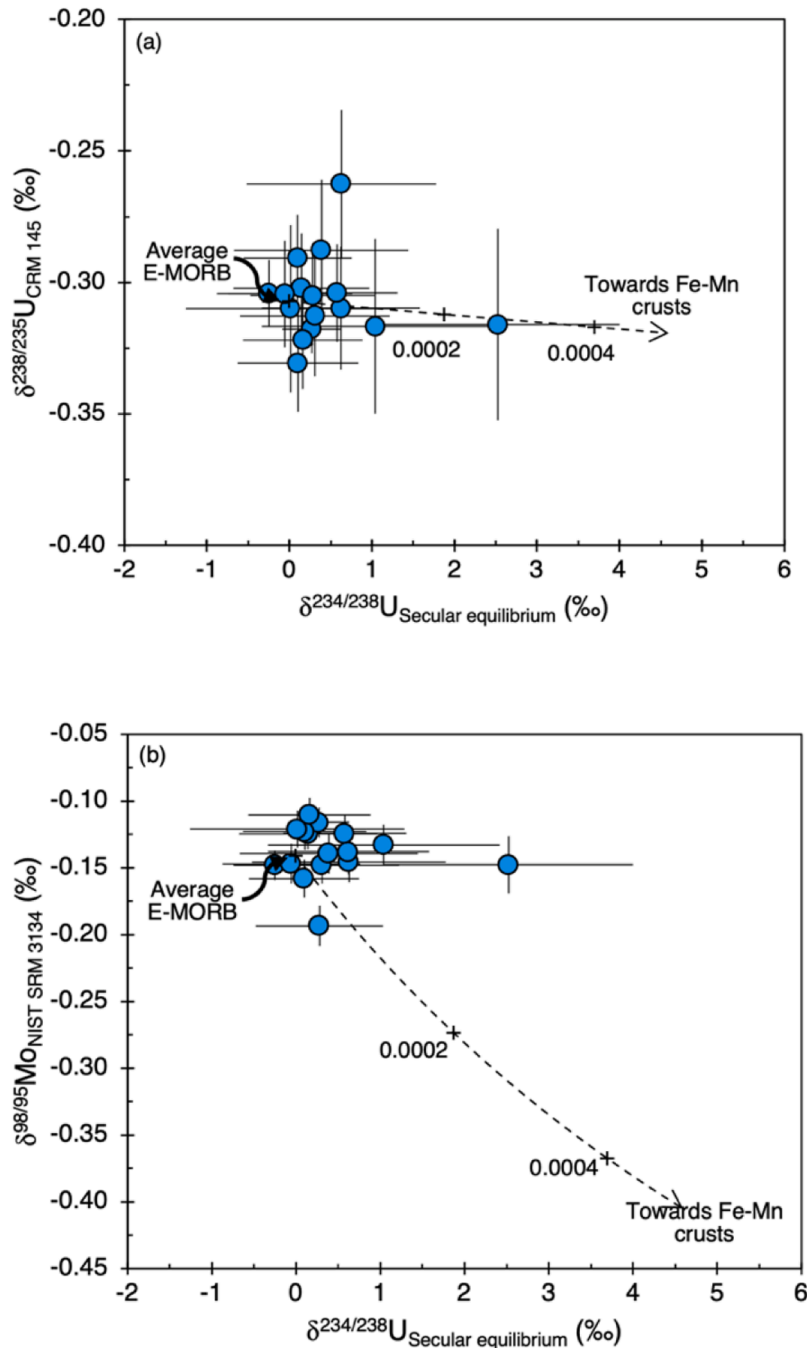


Fig. 4. Modelled mixing curves of $\delta^{234}\text{U}$ versus (a) $\delta^{238}\text{U}$ and (b) $\delta^{98/95}\text{Mo}$, showing the trajectory of Fe-Mn crust addition to our average E-MORB composition (dashed line). Values along the mixing curves show the mass fraction of Fe-Mn crust in the mixture. Compositions used in the mixing calculation are, E-MORB, $\delta^{238}\text{U} = -0.307\text{‰}$, $\delta^{234}\text{U} = 0\text{‰}$, $[\text{U}] = 202\text{ ng g}^{-1}$, $\delta^{98/95}\text{Mo} = -0.14\text{‰}$, and $[\text{Mo}] = 465\text{ ng g}^{-1}$. Fe-Mn crust, $\delta^{238}\text{U} = -0.69\text{‰}$, $\delta^{234}\text{U} = 146.3\text{‰}$, $[\text{U}] = 13100\text{ ng g}^{-1}$, $\delta^{98/95}\text{Mo} = -0.92\text{‰}$, and $[\text{Mo}] = 477000\text{ ng g}^{-1}$ (Henderson and Burton, 1999; Siebert et al., 2003; Goto et al., 2014).

5.3. Recycled crustal material in the E-MORB source

Recent work from Yang et al. (2020) suggests, based on compatible element abundances, that E-MORB geochemistry is explained by the mixture of low degree partial melts of garnet-clinopyroxene pyroxenite (i.e., recycled oceanic crust), with depleted MORB like melts. Melting of this recycled material and mixing with depleted MORB melts generates distinct compositions of element ratios, such as lower Ge/Si, in E-MORB relative to depleted MORB (Yang et al., 2020). The dehydration of subducting slabs during subduction zone processing strips oceanic crust of fluid mobile elements, resulting in high fluid mobile/fluid immobile element ratios in arc lavas. Complementary compositions should then be seen in E-MORB if they contain recycled crustal components, but E-MORB are enriched in both fluid mobile and immobile elements, and have no depletions in elements such as Nb, Tb, and Ti as seen in arc lavas (Niu et al., 2002). To reproduce some of the such E-MORB characteristics in their mixing models, Yang et al. (2020) suggest the recycling of upper continental crust material, that is enriched in elements such as Rb, Ba, and Pb, along with recycled oceanic crust to explain high Rb/Sr, Ba/La, and low Zr/Pb ratios of E-MORB.

Subducted sediments, a proxy for upper continental crust material, are distinctly enriched in Pb and have low Ce/Pb ratios and high $^{207}\text{Pb}/^{204}\text{Pb}$ ratios relative to $^{206}\text{Pb}/^{204}\text{Pb}$ (e.g., White and Dupré, 1986; Plank, 2014). Therefore, we explore the mixing relationships defined by mixing subduction zone processed subducted sediments and recycled oceanic crust (Stracke et al., 2003) into the depleted MORB mantle (DMM) for Pb isotopic compositions and Ce/Pb ratios. Yang et al. (2020) argue for a significant amount of recycled material (in a 95-5 % mixture of recycled oceanic crust and upper continental crust material) mixed into the E-MORB source (e.g., 10 to 30 %). Such amounts of subducting sediment and recycled oceanic crust would decrease the Ce/Pb ratio and increase the $^{207}\text{Pb}/^{204}\text{Pb}$ ratio of the upper mantle source to unobserved compositions (Fig. 5). Recycling of a subducting sediment component, also has implications for the Mo and U isotopic compositions, and current combined Mo-U isotopic data on subducting sediment, and Mo data on metasediments are an unlikely candidate for creating E-MORB, with the meta-/sediment being too isotopically light in $\delta^{98/95}\text{Mo}$ (Frey-muth

et al., 2015; Ahmad et al., 2021) (Fig. 6, 7a). However, we note that sediment compositions can be variable (e.g., Freymuth et al., 2015; Ahmad et al., 2021) and that further characterisation of combined Mo-U isotopic data on subducted sediments is needed to show the potential influence of subducting sediments on the composition of the MORB source. Nonetheless, our inferences from global averaged Ce/Pb and Pb radiogenic compositions still preclude the mixing of subducted sediments into the E-MORB source (Fig. 5).

Other studies also suggest a role for recycled crustal material in the formation of E-MORB sources. Donnelly et al. (2004) argue for low degree partial melts of subducted oceanic crust as eclogite at depth that metasomatises the mantle wedge, creating necessary trace element enrichments. This material is subsequently recirculated through plate motion into the upper mantle over time, ≥ 300 Myr, to allow for radiogenic isotope ratio ingrowth, before being sampled again under MOR's in a larger degree melting event. Our data preclude this model however, as the eclogitic residues of oceanic crust post subduction zone processing have isotopically light $\delta^{98/95}\text{Mo}$ and high Ce/Mo, which is not seen in E-MORB (Chen et al., 2019; Ahmad et al., 2021) (Fig. 7a). This is also likely the case for U given the compositions of volcanic arc lavas and AOC (Fig. 7b). Nielsen et al. (2018) suggest a similar model (i.e., two stage melting, with low degree melt metasomatism, and radiogenic ingrowth followed by sampling under MOR's) but require the addition of subducted sediment, to fit with Ba isotopic data. However, as detailed above, subducted sediments in the E-MORB source are incompatible with Ce/Pb and Pb isotopic data of E-MORB (Fig. 5), as well as with Mo and U elemental and isotopic data (Fig. 6).

Some MORB samples with high "arc-like" $\delta^{98/95}\text{Mo}$, low $(\text{La}/\text{Sm})_{\text{N}}$, and other arc lava geochemical signatures have been linked to mantle sources with substantial contributions from fluid-modified mantle wedge components that formed during subduction processes, such as enrichments in U and Pb that result in lower Nb/U (33) and Ce/Pb (19) (Chen et al., 2025) than canonical mantle values (47 ± 10 and 25 ± 5 respectively) (Hofmann et al., 1986). These MORB samples that preserve so called ghost-arc signatures reflect a way of generating high $\delta^{98/95}\text{Mo}$ in upper mantle MORB sources with recycled crustal components (Chen et al., 2025). However, our E-MORB samples with high $(\text{La}/\text{Sm})_{\text{N}}$ do not

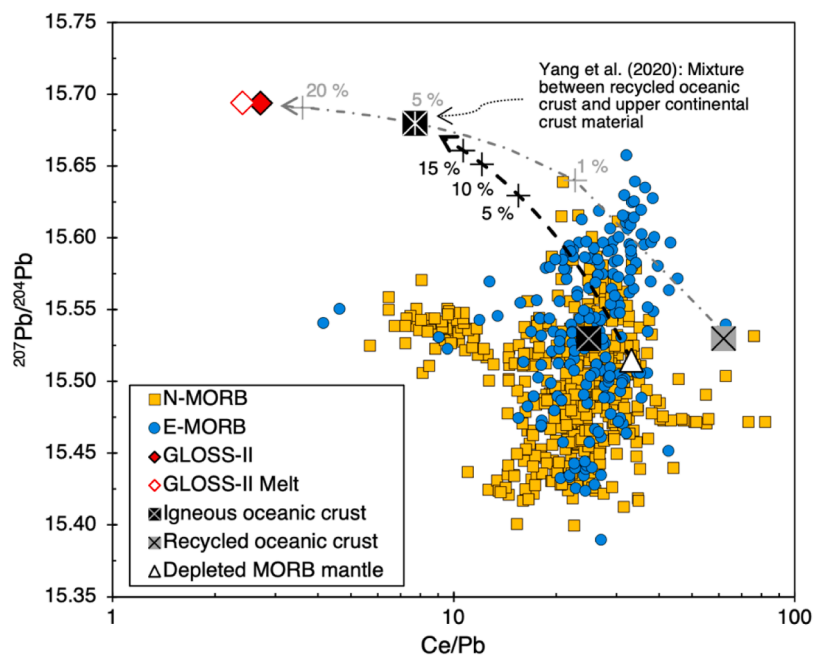


Fig. 5. Mixing model (dashed black line) for $^{207}\text{Pb}/^{204}\text{Pb}$ versus Ce/Pb between the depleted MORB mantle and subduction zone processed recycled oceanic crust mixed with recycled melted sediment (GLOSS-II, Plank, 2014) in a 95-5 % mixture following Yang et al. (2020) (dash-dotted grey line). Composition of recycled oceanic crust and melted subducted sediment composition have been calculated from Stracke et al. (2003). Mixing models have been calculated using parameters and sources in table S8. Filtered global MORB database from Gale et al. (2013) (only including data obtained by ICP-MS methods).

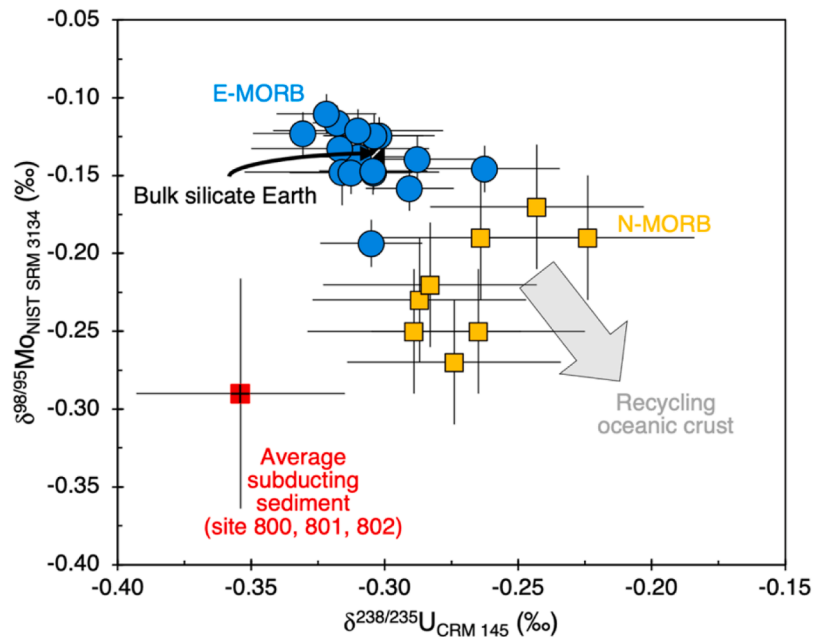


Fig. 6. $\delta^{238}\text{U}$ and $\delta^{98/95}\text{Mo}$ composition of E-MORB samples measured in this work (blue circles) and literature N-MORB (yellow squares) with U and Mo isotopic data. Symbols and sources for literature data are the same as used in Fig. 2. The grey arrow shows the effect of mixing recycled oceanic crust into the mantle, which does not explain the composition of E-MORB relative to N-MORB.

show evidence of arc lava signatures. For example they have average Nb/U (48) and Ce/Pb (28) near canonical mantle values (Hofmann et al., 1986). Therefore, the high $\delta^{98/95}\text{Mo}$ of our E-MORB samples cannot be explained by recycled fluid-modified mantle components.

The simplest interpretation of our new E-MORB data from the North Atlantic Ocean is that they do not contain a recycled, subduction zone processed, crustal component (Figs. 6, 7). Therefore, we argue for a model that does not invoke recycled crustal material to explain the Mo and U elemental and isotopic compositions of E-MORB samples.

5.4. Low degree partial melting and mantle metasomatism

Low degree partial melting has been suggested to explain the incompatible element enrichment of fluid and non-fluid mobile elements in the E-MORB source (e.g., Niu et al., 2002). Uranium is highly incompatible during mantle melting, $D_{\text{Cpx/melt}} \text{U}^{4+} \sim 0.02$ (Fonseca et al., 2014), and therefore, any potential isotopic fractionation between melt and initial source from partial melting of peridotite will be insignificant as virtually all U will enter the melt. The lower $\delta^{238}\text{U}$ of E-MORB than N-MORB can therefore not be explained by isotopic fractionation during partial melting. The $\delta^{238}\text{U}$ compositions of our E-MORB samples thus represent the compositions of their upper mantle sources. Their chondritic values reflect mantle compositions little- or un-affected by the recycling of AOC since the onset of oxic deep oceans (~ 600 Ma), which has been argued to increase the $\delta^{238}\text{U}$ of the upper mantle as sampled by N-MORB (Andersen et al., 2015). We suggest that our $\delta^{238}\text{U}$ compositions of E-MORB can hence be explained by a model where ancient (≥ 600 Ma) mantle components are preserved and unaffected by more recent (< 600 Ma) crustal recycling.

This is compatible with a model of low degree partial melting and peridotite metasomatism, as outlined in Niu et al. (2002), and applied from a Mo isotopic perspective in Chen et al. (2022) and for other isotope systems such as Fe (e.g., Guo et al., 2023). Enriched domains in the upper mantle could exist as volumetrically minor lithologies of low degree melts dispersed as (frozen) dykes or veins in a depleted peridotitic matrix (Niu et al., 2002). Low degree melting may occur at the boundary between the thickening and cooling oceanic lithosphere and the asthenosphere. This region is marked by a low velocity zone (e.g.,

Green, 1971; Niu et al., 2002), which likely reflects the presence of small amounts of melt (e.g., Hirschmann, 2010). These small degree, low volume melts would have low thermal inertia, and will freeze as they migrate into the base of the oceanic lithosphere (McKenzie, 1989). Such metasomatised lithosphere has also been invoked in the source of some alkaline lavas (e.g., Pilet et al., 2008). The existence of alkali volcanism with a chemistry that reflects small degree melting in the presence of garnet, far from any plate boundary or hot-spot in the north-western Pacific plate (Petit spots) (Hirano et al., 2006), has been used as evidence of small degree melts that are actively forming in the modern asthenosphere. The Petit spots anomalously result in a surface expression of this process due to lithospheric fractures from plate flexure during subduction allowing the melts to ascend (Hirano et al., 2006).

Uranium isotopic data of E-MORB samples requires that the initial low degree melting event happened ≥ 600 Ma, metasomatising the uppermost mantle and freezing in upper mantle compositions with enriched trace element compositions and chondritic $\delta^{238}\text{U}$. Thus, domains enriched in U are isolated from the evolution of ambient upper mantle to higher $\delta^{238}\text{U}$ by recycling of oceanic crust altered in oxic deep ocean conditions (< 600 Ma). A full mechanistic explanation of the model of recycling and mixing of metasomatised oceanic lithosphere into the mantle is not the aim of our work and we refer readers to Niu et al. (2002) and Niu and O'Hara (2003) for details. In brief, these metasomatised portions of the oceanic lithosphere would be subducted, and since they are in deep portions of lithosphere, they would not undergo dehydration. Heating of this material increases its buoyancy, and the crust and mantle separate by buoyancy contrast with crust sinking and thermally buoyant peridotitic mantle rising with metasomatised sections of dykes and veins (Niu et al., 2002; Niu and O'Hara, 2003). Such metasomatised lithosphere is stirred into the upper mantle but remains chemically distinct until ultimately sampled by melting beneath ridges to give rise to E-MORB (Fig. 8) (Niu et al., 2002; Niu and O'Hara, 2003).

Molybdenum isotope data of E-MORB are also compatible with such a model (Chen et al., 2022), but unlike U, the Mo isotopic compositions of E-MORB may be fractionated from its source. In pyroxene, the major upper mantle Mo host, Mo sits in the octahedral M1 site (Leitzke et al., 2017), while in melt Mo^{6+} is coordinated tetrahedrally (Holzheid et al.,

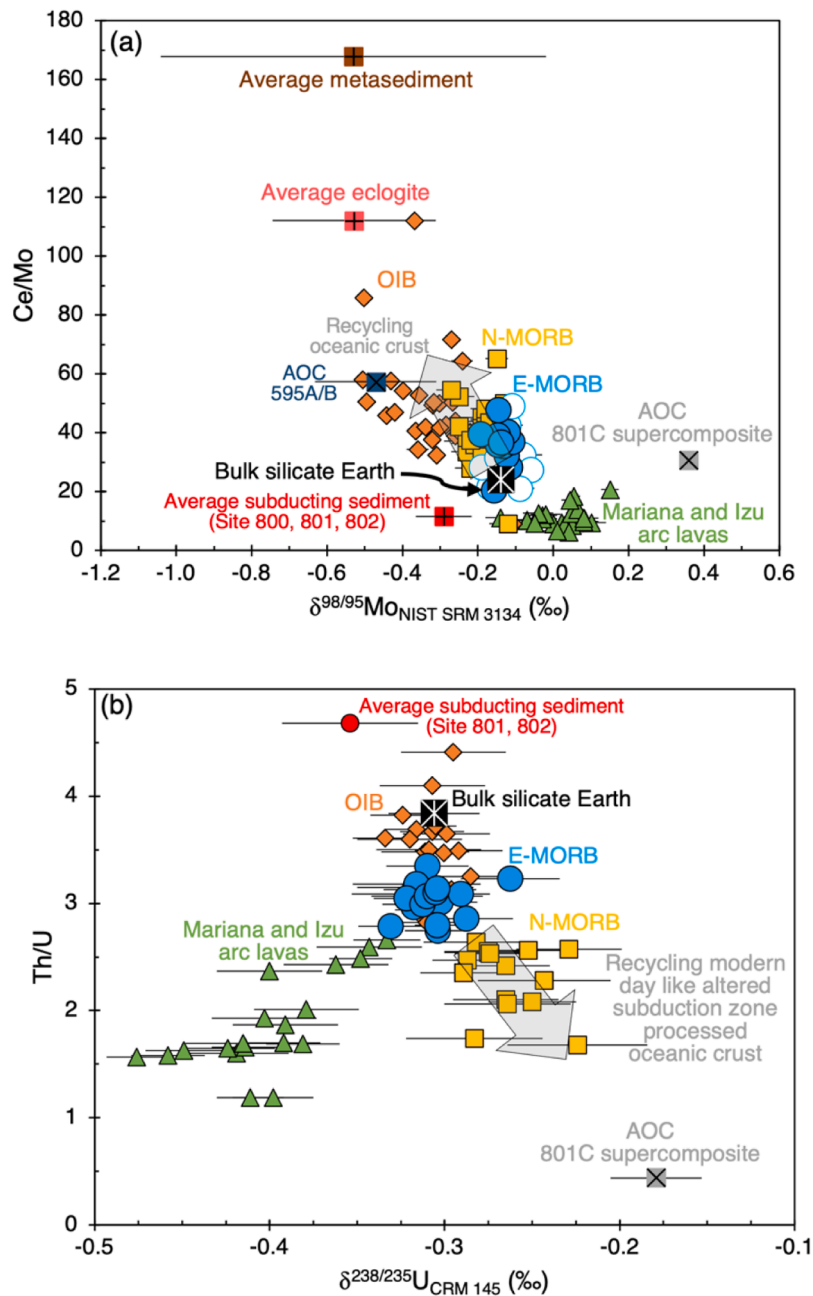


Fig. 7. (a) $\delta^{98/95}\text{Mo}$ and (b) $\delta^{238}\text{U}$ versus Ce/Mo and Th/U for N-MORB, E-MORB, AOC, Mariana and Izu arc lavas, OIB, eclogite, and subducting sediment and metasediment. Symbols and sources for literature data are the same as used in figure 2. Literature E-MORB data, shown as hollow blue circles, are from Bezard et al. (2016), Chen et al. (2022) and Hin et al. (2022). Grey arrows show the effect of mixing recycled oceanic crust into the upper mantle, which does not account for the composition of E-MORB.

1994; O'Neill and Eggins, 2002; Farges et al., 2006). While a minor species at modern ambient upper mantle oxygen fugacity, Mo^{4+} is significantly less incompatible than Mo^{6+} in pyroxenes ($D_{\text{Cpx/melt}} \text{Mo}^{4+} = \sim 2$) (Leitzke et al., 2017) and is coordinated octahedrally in both mineral and melt (Farges et al., 2006). Heavier isotopes are concentrated in phases with stiffer and stronger bonds, which form between ions with lower co-ordination number and higher valence state (e.g., Schauble, 2004). Melts are therefore predicted to become isotopically heavier in Mo than residues during partial melting (McCoy-West et al., 2019). The fractionation between Mo isotopes becomes larger at smaller degrees of melting and lower $\text{Mo}^{6+}/\text{Mo}_T$ (Mo total) ratios (i.e., more reduced compositions, unlikely for modern oxidised mantle) (Fig. S7a). Chen et al. (2022), following the melting models of McCoy-West et al. (2019), proposed that at low degrees of melting, $\sim 0.2\%$ of modern-day

depleted mantle, $\delta^{98/95}\text{Mo} = -0.2\%$ (Hin et al., 2022), at a modern-day redox state, $\text{Mo}^{6+}/\text{Mo}_T = 0.99$ (O'Neill and Eggins, 2002), results in a melt composition, $\delta^{98/95}\text{Mo} = \sim -0.01\%$ and $(\text{La}/\text{Sm})_N \sim 5.4$, that is sufficient to explain the high $\delta^{98/95}\text{Mo}$ values and chemical enrichments seen in global E-MORB when mixed with a depleted MORB component (Fig. 9a).

However, we find that with our new data on E-MORB the resulting isotopic compositions from such low degree melting are too isotopically heavy to explain some of our data, even at higher $\text{Mo}^{6+}/\text{Mo}_T$ ratios, ~ 0.999 (Fig. 9a). McCoy-West et al. (2019) used the 'ionic model' and literature bond length data to derive a fractionation factor between ^{98}Mo and ^{95}Mo during mantle partial melting, $\alpha^{98/95}\text{Mo}_{\text{Melt-Silicate}} \sim 0.99977$. Such a value has not been directly, experimentally verified and notably predicts larger fractionation than for another redox sensitive system Cr

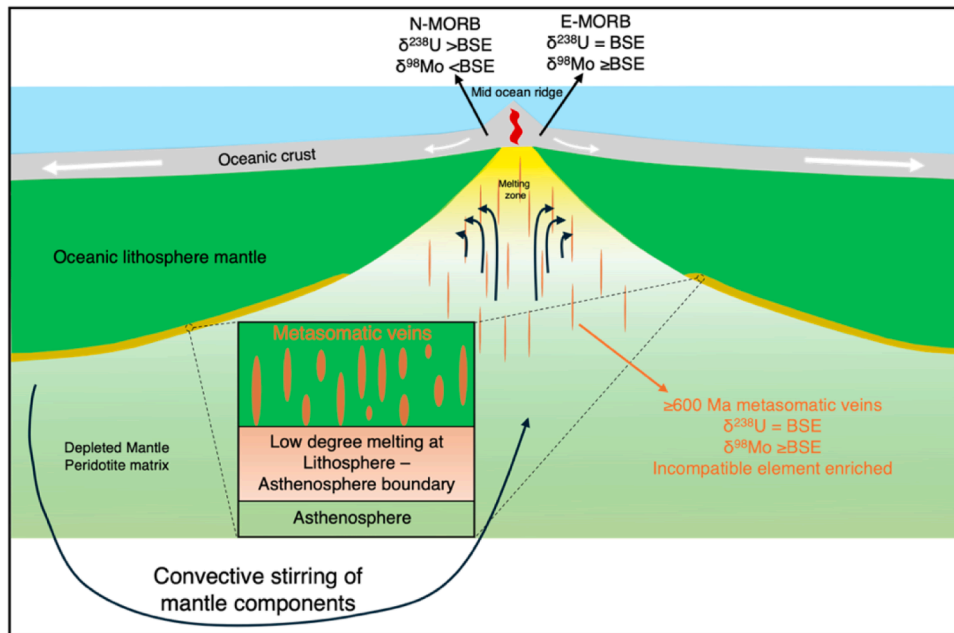


Fig. 8. Cartoon schematic of E-MORB source formation based on and modified from Niu et al. (2002) and Guo et al. (2023). Low degree partial melts enriched in incompatible elements (orange lenses) form ≥ 600 Ma in the low velocity zone at the boundary between the lithosphere and asthenosphere (shaded orange region at base of oceanic lithosphere mantle) and become trapped by migration and freezing in the cooling and thickening overlying oceanic lithosphere. These components preserve older mantle compositions with BSE $\delta^{238}\text{U}$. As oceanic lithosphere is subducted, the metasomatised lithosphere is stirred back into the upper mantle and some is entrained beneath MOR's and melts to produce E-MORB.

(e.g., Jerram et al., 2022) for example. We note that our data imply a smaller melt-silicate fractionation of Mo isotopes, and we illustrate this using $\alpha^{98/95}\text{Mo}_{\text{Melt-Silicate}}$ of 0.9999 (Fig. S7b, 9b). Experimental work is required to assess if this empirical reassessment of the fractionation factor is justified.

Our model fit to $\delta^{98/95}\text{Mo}$ data is further improved given inferences from $\delta^{238}\text{U}$ compositions of E-MORB that imply the initial low degree melts form not from a modern-day depleted mantle, but ancient ≥ 600 Ma depleted mantle compositions (Fig. 8). Isotopic perturbation of Mo in the upper mantle by crustal recycling is inferred to have occurred for longer timescales than for U. Hin et al. (2022) show that at least ~ 1 to 1.4 Gyr of oceanic crust recycling is needed to lower the $\delta^{98/95}\text{Mo}$ value of the upper mantle from -0.14 ‰ (BSE) to -0.2 ‰ (modern-day depleted upper mantle). Although, as we note, if the melt-silicate fractionation of Mo isotope is smaller than estimated by McCoy-West et al. (2019), these timescales would be shorter, which is possible, as the U isotopic composition of N-MORB suggests that upper mantle compositions can be perturbed by recycled crust within 600 Myr. The isolation of small degree melts from a convecting upper mantle at various ages ≥ 600 Ma can help explain the variably elevated $\delta^{98/95}\text{Mo}$ of global E-MORB. We show this on Fig. 9b, where low degree melt compositions form from an upper mantle less affected by crustal recycling with higher $\delta^{98/95}\text{Mo}$ than modern day, resulting in an enriched melt end member composition of $\delta^{98/95}\text{Mo} \sim -0.1$ ‰ and $(\text{La}/\text{Sm})_{\text{N}} \sim 5.4$ at $\text{Mo}^{6+}/\text{Mo}_{\text{T}} = 0.99$.

In summary, the metasomatism of depleted, oceanic lithosphere with low degree melts formed ≥ 600 Ma would create a source dominated by a U-rich component with $\delta^{238}\text{U} \approx \text{BSE}$ and a range of $\delta^{98/95}\text{Mo}$ compositions $\geq \text{BSE}$, with variable enrichment in $(\text{La}/\text{Sm})_{\text{N}}$ (Fig. 8). Low degree melting would also create variable degrees of enrichment in other chemical tracers of enrichment, such as Nb/Zr, Th/Yb, and Sm/Nd, that also show trends with $\delta^{238}\text{U}$ and $\delta^{98/95}\text{Mo}$, that distinguish E-MORB from N-MORB (Fig. S8). This enriched component, when stirred back into the upper mantle and sampled by melting beneath a MOR in a larger degree melting event, can explain the chemical compositions of non-hot-spot influenced E-MORB (Figs. 3c, d, 9b). The timescale of ≥ 600 Ma inferred for this recycling process is about twice as long as the residence

time of E-MORB sources calculated by Donnelly et al. (2004) from radiogenic isotope pseudo-chrons. It will be of interest to rationalise these different timescales using a consistent set of radiogenic isotope and $\delta^{238}\text{U}$ measurements on the same samples, which is currently not possible.

6. Conclusions

A set of hand-picked E-MORB glasses from the Northern mid-Atlantic ridge picked to different degrees of stringency all have $^{234}\text{U}/^{238}\text{U}$ ratios close to secular equilibrium, indicating that samples likely reflect primary U and Mo isotopic composition. These E-MORB samples show a limited range of $\delta^{238}\text{U}$ and $\delta^{98/95}\text{Mo}$ from ~ -0.33 to -0.26 ‰ and -0.19 to -0.11 ‰ respectively and are both, on average, indistinguishable from the bulk silicate Earth (chondritic) U and Mo isotopic compositions. These E-MORB therefore have contrasting sources to modern N-MORB, which are super-chondritic in U and sub-chondritic in Mo isotope ratios, thought to be due to the recycling of modern day like subduction zone processed altered oceanic crust (Andersen et al., 2015; Hin et al., 2022). Our E-MORB data are inconsistent with models that explain their enrichment with recycled oceanic crust and or recycled sediment (e.g., Allègre and Turcotte, 1986; Prinzhofer et al., 1989; Donnelly et al., 2004; Hémond et al., 2006; Waters et al., 2011; Ulrich et al., 2012; Nielsen et al., 2018; Yang et al., 2020) but are consistent with a model of recycled oceanic lithospheric mantle, metasomatised by small degree asthenosphere melts (Niu et al., 2002; Chen et al., 2022; Guo et al., 2023). This process effectively isolates the composition of the upper mantle at the time of the small degree melting until the metasomatised sources are resampled as E-MORB by melting beneath ridges. Uranium isotopic compositions (which are not affected by low degree partial melting) show that this initial low degree melting event occurred in an upper mantle with a chondritic $\delta^{238}\text{U}$, namely prior to its contamination with isotopically heavy recycled altered oceanic crust. This corresponds to an age ≥ 600 Ma, set by the estimated timing of deep ocean oxygenation (Andersen et al., 2015), providing a minimum bound on the antiquity of the E-MORB source. Molybdenum isotopic

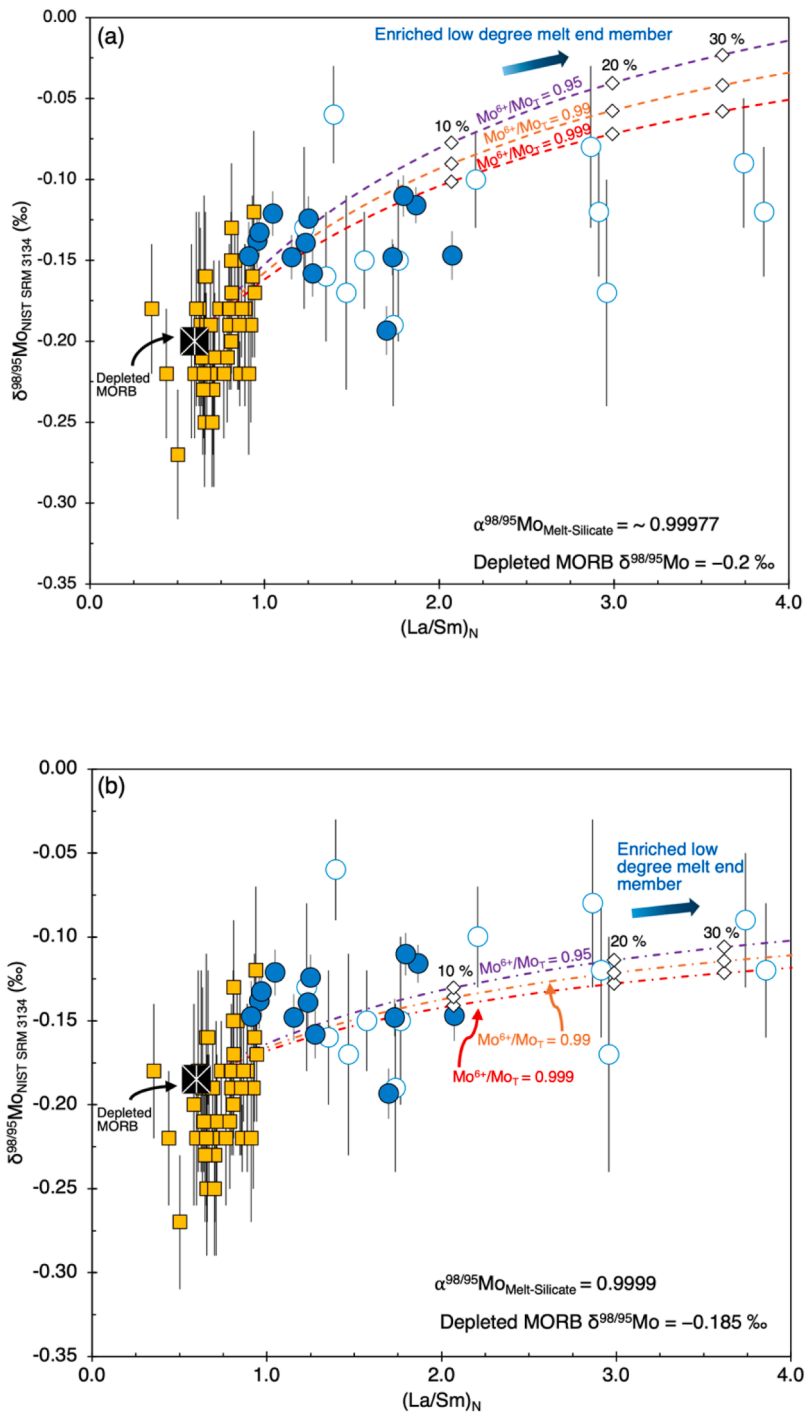


Fig. 9. Non-modal, batch melting modelling of $(La/Sm)_N$ and Mo isotopic composition of melt. Mixing lines are shown between a depleted MORB (represented by 20 % melting of DMM) and an enriched low degree melt end member generated by 0.2 % melting of DMM at different mantle fO_2 ($Mo^{6+}/Mo_T = 0.999$ to 0.95). Symbols and sources for data are the same as used in figure 2. Model calculations follow McCoy-West et al. (2019) and Chen et al. (2022). Parameters used are given in table S9. White diamonds indicate mixing proportions. (a) $\alpha^{98/95}Mo_{Melt-Silicate} \sim 0.99977$, Depleted MORB $\delta^{98/95}Mo = -0.2$ ‰ (b) $\alpha^{98/95}Mo_{Melt-Silicate} \sim 0.9999$, Depleted MORB $\delta^{98/95}Mo = -0.185$ ‰.

compositions of global E-MORB are compatible with such a model but are also potentially fractionated during low degree partial melting to isotopically heavier compositions (McCoy-West et al., 2019; Chen et al., 2022).

Data availability

Data are available through Mendeley data at: <https://data.mendeley.com/datasets/wm84d8m8js/2>.

[com/datasets/wm84d8m8js/2](https://data.mendeley.com/datasets/wm84d8m8js/2).

CRediT authorship contribution statement

Joel B. Rodney: Writing – review & editing, Writing – original draft, Visualization, Validation, Project administration, Methodology, Investigation, Formal analysis, Data curation, Conceptualization. **Morten B. Andersen:** Writing – review & editing, Supervision, Project

administration, Funding acquisition, Conceptualization. **Bramley J. Murton**: Writing – review & editing, Resources. **Tim Elliott**: Writing – review & editing, Supervision, Project administration, Funding acquisition, Conceptualization.

Declaration of competing interest

The authors declare that they have no known competing financial interests or personal relationships that could have appeared to influence the work reported in this paper.

Acknowledgments

JBR would like to acknowledge Christopher D. Coath and Carolyn Taylor for the upkeep of the labs. JBR would like to acknowledge Ian Parkinson, Paul Savage, and Shuo Chen for useful comments. JBR would like to thank Paolo A. Sossi for providing melting models. JBR would like to thank Fang-Zhen Teng for editorial handling and Qasid Ahmad and one anonymous reviewer for helpful comments. JBR was supported by a NERC GW4 + Doctoral Training Partnership studentship from the Natural Environmental Research Council [NE/S007504/1]. JBR, MBA, and TE acknowledge funding from a NERC grant [NE/T012595/1 & NE/T012633/1]. RSS James Cook cruise JC024 expedition and project were funded by NERC award NE/C520598/1 (Roger Searle at Durham University) and NE/C520612/1 (Bramley J Murton at the National Oceanography Centre).

Supplementary materials

Supplementary material associated with this article can be found, in the online version, at [doi:10.1016/j.epsl.2025.119491](https://doi.org/10.1016/j.epsl.2025.119491).

References

- Ahmad, Q., Wille, M., König, S., Rosca, C., Hensel, A., Pettke, T., Hermann, J., 2021. The molybdenum isotope subduction recycling conundrum: a case study from the Tongan subduction zone, Western Alps and Alpine Corsica. *Chem. Geol.* 576, 120231.
- Allègre, C.J., Turcotte, D.L., 1986. Implications of a two-component marble-cake mantle. *Nature* 323, 123–127.
- Andersen, M.B., Romaniello, S., Vance, D., Little, S.H., Herdman, R., Lyons, T.W., 2014. A modern framework for the interpretation of $^{238}\text{U}/^{235}\text{U}$ in studies of ancient ocean redox. *Earth. Planet. Sci. Lett.* 400, 184–194.
- Andersen, M.B., Elliott, T., Freymuth, H., Sims, K.W.W., Niu, Y., Kelley, K.A., 2015. The terrestrial uranium isotope cycle. *Nature* 517, 356–359.
- Andersen, M.B., Rodney, J.B., Freymuth, H., Vils, F., Harris, M., Cooper, K., Teagle, D.A.H., Elliott, T., 2024. Time scales and mechanisms of uranium uptake in altered ocean crust; observations from the ~15 million year-old site 1256 in the eastern equatorial Pacific. *Geochim. Cosmochim. Acta* 382, 142–159.
- Bezard, R., Fischer-Gödde, M., Hamelin, C., Brennecke, G.A., Kleine, T., 2016. The effects of magmatic processes and crustal recycling on the molybdenum stable isotopic composition of Mid-Ocean Ridge Basalts. *Earth. Planet. Sci. Lett.* 453, 171–181.
- Bougault, H., Dmitriev, L., Schilling, J.G., Sobolev, A., Joron, J.L., Needham, H.D., 1988. Mantle heterogeneity from trace elements: MAR triple junction near 14°N. *Earth. Planet. Sci. Lett.* 88, 27–36.
- Burkhardt, C., Hin, R.C., Kleine, T., Bourdon, B., 2014. Evidence for Mo isotope fractionation in the solar nebula and during planetary differentiation. *Earth. Planet. Sci. Lett.* 391, 201–211.
- Chen, S., Sun, P., Niu, Y., Guo, P., Elliott, T., Hin, R.C., 2022. Molybdenum isotope systematics of lavas from the East Pacific Rise: constraints on the source of enriched mid-ocean ridge basalt. *Earth. Planet. Sci. Lett.* 578, 117283.
- Chen, S., Hin, R.C., John, T., Brooker, R., Bryan, B., Niu, Y., Elliott, T., 2019. Molybdenum systematics of subducted crust record reactive fluid flow from underlying slab serpentine dehydration. *Nat. Commun.* 10, 4773.
- Chen, Z., Teng, F.-Z., Stern, R.J., Zhang, Y., Li, J., Zeng, Z., 2025. Molybdenum isotope evidence for subduction-modified mantle beneath mid-ocean ridges. *Earth. Planet. Sci. Lett.* 658, 119294.
- Cheng, H., Edwards, R.L., Shen, C.-C., Polyak, V.J., Asmerom, Y., Woodhead, J., Hellstrom, J., Wang, Y., Kong, X., Spötl, C., Wang, X., Alexander, E.C., 2013. Improvements in ^{230}Th dating, ^{230}Th and ^{234}U half-life values, and U–Th isotopic measurements by multi-collector inductively coupled plasma mass spectrometry. *Earth. Planet. Sci. Lett.* 371–372, 82–91.
- Collerson, K.D., Kamber, B.S., 1999. Evolution of the continents and the atmosphere inferred from Th–U–Nb systematics of the depleted mantle. *Science* (1979) 283, 1519–1522.
- Donnelly, K.E., Goldstein, S.L., Langmuir, C.H., Spiegelman, M., 2004. Origin of enriched ocean ridge basalts and implications for mantle dynamics. *Earth. Planet. Sci. Lett.* 226, 347–366.
- Elliott, T., Zindler, A., Bourdon, B., 1999. Exploring the kappa conundrum: the role of recycling in the lead isotope evolution of the mantle. *Earth. Planet. Sci. Lett.* 169, 129–145.
- Farges, F., Siewert, R., Brown, G., Guesdon, A., Morin, G., 2006. Structural environments around molybdenum in silicate glasses and melts. I. Influence of composition and oxygen fugacity on the local structure of molybdenum. *Can. Mineral.* 44, 731–753.
- Fonseca, R.O.C., Mallmann, G., Sprung, P., Sommer, J., Heuser, A., Speelmanns, I.M., Blanchard, H., 2014. Redox controls on tungsten and uranium crystal/silicate melt partitioning and implications for the U/W and Th/W ratio of the lunar mantle. *Earth. Planet. Sci. Lett.* 404, 1–13.
- Freymuth, H., Andersen, M.B., Elliott, T., 2019. Uranium isotope fractionation during slab dehydration beneath the Izu arc. *Earth. Planet. Sci. Lett.* 522, 244–254.
- Freymuth, H., Vils, F., Willbold, M., Taylor, R.N., Elliott, T., 2015. Molybdenum mobility and isotopic fractionation during subduction at the Mariana arc. *Earth. Planet. Sci. Lett.* 432, 176–186.
- Gale, A., Dalton, C.A., Langmuir, C.H., Su, Y., Schilling, J.-G., 2013. The mean composition of ocean ridge basalts: geochemistry. *Geophys., Geosyst.* 14, 489–518.
- Gaschnig, R.M., Reinhard, C.T., Planavsky, N.J., Wang, X., Asael, D., Chauvel, C., 2017. The Molybdenum isotope system as a tracer of slab input in subduction zones: an example from Martinique, Lesser Antilles Arc. *Geochem., Geophys., Geosyst.* 18, 4674–4689.
- Goto, K.T., Anbar, A.D., Gordon, G.W., Romaniello, S.J., Shimoda, G., Takaya, Y., Tokumaru, A., Nozaki, T., Suzuki, K., Machida, S., Hanyu, T., Usui, A., 2014. Uranium isotope systematics of ferromanganese crusts in the Pacific Ocean: implications for the marine $^{238}\text{U}/^{235}\text{U}$ isotope system. *Geochim. Cosmochim. Acta* 146, 43–58.
- Green, D.H., 1971. Composition of basaltic magmas as indicators of conditions of origin: application to oceanic volcanism. *Philos. Trans. R. Soc. Lond. Ser. A* 268, 707–722.
- Guo, P., Niu, Y., Chen, S., Duan, M., Sun, P., Chen, Y., Gong, H., Wang, X., 2023. Low-degree melt metasomatic origin of heavy Fe isotope enrichment in the MORB mantle. *Earth. Planet. Sci. Lett.* 601, 117892.
- Gutjahr, M., Frank, M., Stirling, C.H., Klemm, V., van de Flierdt, T., Halliday, A.N., 2007. Reliable extraction of a deepwater trace metal isotope signal from Fe–Mn oxyhydroxide coatings of marine sediments. *Chem. Geol.* 242, 351–370.
- Halliday, A.N., Lee, D.-C., Tommasini, S., Davies, G.R., Paslick, C.R., Godfrey Fitton, J., James, D.E., 1995. Incompatible trace elements in OIB and MORB and source enrichment in the sub-oceanic mantle. *Earth. Planet. Sci. Lett.* 133, 379–395.
- Hémond, C., Hofmann, A.W., Vlastélic, I., Nauret, F., 2006. Origin of MORB enrichment and relative trace element compatibilities along the Mid-Atlantic Ridge between 10° and 24°N. *Geochem., Geophys., Geosyst.* 7, Q12010.
- Henderson, G.M., Burton, K.W., 1999. Using ($^{234}\text{U}/^{238}\text{U}$) to assess diffusion rates of isotope tracers in ferromanganese crusts. *Earth. Planet. Sci. Lett.* 170, 169–179.
- Hin, R.C., Hibbert, K.E.J., Chen, S., Willbold, M., Andersen, M.B., Kiseeva, E.S., Wood, B. J., Niu, Y., Sims, K.W.W., Elliott, T., 2022. The influence of crustal recycling on the molybdenum isotope composition of the Earth's mantle. *Earth. Planet. Sci. Lett.* 595, 117760.
- Hirano, N., Takahashi, E., Yamamoto, J., Abe, N., Ingle, S.P., Kaneoka, I., Hirata, T., Kimura, J.-I., Ishii, T., Ogawa, Y., Machida, S., Suyehiro, K., 2006. Volcanism in response to plate flexure. *Science* (1979) 313, 1426–1428.
- Hirschmann, M.M., 2010. Partial melt in the oceanic low velocity zone. *Phys. Earth Planetary Interiors* 179, 60–71.
- Hofmann, A.W., Jochum, K.P., Seufert, M., White, W.M., 1986. Nb and Pb in oceanic basalts: new constraints on mantle evolution. *Earth. Planet. Sci. Lett.* 79, 33–45.
- Holzheid, A., Borisov, A., Palme, H., 1994. The effect of oxygen fugacity and temperature on solubilities of nickel, cobalt, and molybdenum in silicate melts. *Geochim. Cosmochim. Acta* 58, 1975–1981.
- Jerram, M., Bonnard, P., Harvey, J., Ionov, D., Halliday, A.N., 2022. Stable chromium isotopic variations in peridotite mantle xenoliths: metasomatism versus partial melting. *Geochim. Cosmochim. Acta* 317, 138–154.
- Kipp, M.A., Li, H., Ellwood, M.J., John, S.G., Middag, R., Adkins, J.F., Tissot, F.L.H., 2022. ^{238}U , ^{235}U and ^{234}U in seawater and deep-sea corals: a high-precision reappraisal. *Geochim. Cosmochim. Acta* 336, 231–248.
- König, S., Wille, M., Voegelin, A., Schoenberg, R., 2016. Molybdenum isotope systematics in subduction zones. *Earth. Planet. Sci. Lett.* 447, 95–102.
- Kostopoulos, D.K., Murton, B.J., 1992. Origin and distribution of components in boninite genesis: significance of the OIB component. *Geol. Soc., Lond., Spec. Publ.* 60, 133–154.
- Leitzke, F.P., Fonseca, R.O.C., Sprung, P., Mallmann, G., Lagos, M., Michely, L.T., Münker, C., 2017. Redox dependent behaviour of molybdenum during magmatic processes in the terrestrial and lunar mantle: implications for the Mo/W of the bulk silicate Moon. *Earth. Planet. Sci. Lett.* 474, 503–515.
- Liang, Y.-H., Halliday, A.N., Siebert, C., Fitton, J.G., Burton, K.W., Wang, K.-L., Harvey, J., 2017. Molybdenum isotope fractionation in the mantle. *Geochim. Cosmochim. Acta* 199, 91–111.
- Lyons, T.W., Reinhard, C.T., Planavsky, N.J., 2014. The rise of oxygen in Earth's early ocean and atmosphere. *Nature* 506, 307–315.
- Maia, M., Goslin, J., Gente, P., 2007. Evolution of the accretion processes along the Mid-Atlantic Ridge north of the Azores since 5.5 Ma: an insight into the interactions between the ridge and the plume. *Geochem., Geophys., Geosyst.* 8, Q03013.
- McCoy-West, A.J., Chowdhury, P., Burton, K.W., Sossi, P., Nowell, G.M., Fitton, J.G., Kerr, A.C., Cawood, P.A., Williams, H.M., 2019. Extensive crustal extraction in Earth's early history inferred from molybdenum isotopes. *Nat. Geosci.* 12, 946–951.

- McCulloch, M.T., 1993. The role of subducted slabs in an evolving Earth. *Earth. Planet. Sci. Lett.* 115, 89–100.
- McDonough, W.F., Sun, S.-S., 1995. The composition of the Earth. *Chem. Geol.* 120, 223–253.
- McKenzie, D., 1989. Some remarks on the movement of small melt fractions in the mantle. *Earth. Planet. Sci. Lett.* 95, 53–72.
- Nielsen, S.G., Horner, T.J., Pryer, H.V., Blusztajn, J., Shu, Y., Kurz, M.D., Roux, V.L., 2018. Barium isotope evidence for pervasive sediment recycling in the upper mantle. *Sci. Adv.* 4, eaas8675.
- Niu, Y., O'Hara, M.J., 2003. Origin of ocean island basalts: a new perspective from petrology, geochemistry, and mineral physics considerations: origin of ocean island basalts. *J. Geophys. Res.* 108, 2209.
- Niu, Y., Regelous, M., Wendt, I.J., Batiza, R., O'Hara, M.J., 2002. Geochemistry of near-EPR seamounts: importance of source vs. process and the origin of enriched mantle component. *Earth. Planet. Sci. Lett.* 199, 327–345.
- O'Neill, H.S.C., Eggins, S.M., 2002. The effect of melt composition on trace element partitioning: an experimental investigation of the activity coefficients of FeO, NiO, CoO, MoO₂ and MoO₃ in silicate melts. *Chem. Geol.* 186, 151–181.
- Pilet, S., Baker, M.B., Stolper, E.M., 2008. Metasomatized lithosphere and the origin of alkaline Lavas. *Science* (1979) 320, 916–919.
- Plank, T., 2014. 4.17 - The chemical composition of subducting sediments. In: Holland, H.D., Turekian, K.K. (Eds.), *Treatise on Geochemistry* (Second Edition). Elsevier, pp. 607–629.
- Prinzhofer, A., Lewin, E., Allègre, C.J., 1989. Stochastic melting of the marble cake mantle: evidence from local study of the East Pacific Rise at 12°50'N. *Earth. Planet. Sci. Lett.* 92, 189–206.
- Reinitz, L., Turekian, K.K., 1989. 230Th/238U and 226Ra/230Th fractionation in young basaltic glasses from the East Pacific Rise. *Earth. Planet. Sci. Lett.* 94, 199–207.
- Richter, S., Alonso-Munoz, A., Eykens, R., Jacobsson, U., Kuehn, H., Verbruggen, A., Aregbe, Y., Wellum, R., Keegan, E., 2008. The isotopic composition of natural uranium samples - measurements using the new n(²³³U)/n(²³⁶U) double spike IRMM-3636. *Int. J. Mass Spectrom.* 269, 145–148.
- Schauble, E.A., 2004. Applying stable isotope fractionation theory to new systems. *Rev. Mineral. Geochem.* 55, 65–111.
- Schilling, J.G., Thompson, G., Kingsley, R., Humphris, S., 1985. Hotspot—Migrating ridge interaction in the South Atlantic. *Nature* 313, 187–191.
- Schilling, J.-G., 1975. Rare-Earth variations across 'normal segments' of the Reykjanes Ridge, 60°–53'N, Mid-Atlantic Ridge, 29°S, and East Pacific Rise, 2°–19°S, and evidence on the composition of the underlying low-velocity layer. *J. Geophys. Res.* 80, 1459–1473.
- Searle, R.C., Murton, B.J., Achenbach, K., LeBas, T., Tivey, M., Yeo, I., Cormier, M.H., Carlu, J., Ferreira, P., Mallows, C., Morris, K., Schroth, N., van Calsteren, P., Waters, C., 2010. Structure and development of an axial volcanic ridge: Mid-Atlantic Ridge, 45°N. *Earth. Planet. Sci. Lett.* 299, 228–241.
- Siebert, C., Nägler, T.F., von Blanckenburg, F., Kramers, J.D., 2003. Molybdenum isotope records as a potential new proxy for paleoceanography. *Earth. Planet. Sci. Lett.* 211, 159–171.
- Staudigel, H., Davies, G.R., Hart, S.R., Marchant, K.M., Smith, B.M., 1995. Large scale isotopic Sr, Nd and O isotopic anatomy of altered oceanic crust: DSDP/ODP sites 417/418. *Earth. Planet. Sci. Lett.* 130, 169–185.
- Stracke, A., Bizimis, M., Salters, V.J.M., 2003. Recycling oceanic crust: quantitative constraints. *Geochem., Geophys., Geosyst.* 4, 8003.
- Ulrich, M., Hémond, C., Nonnotte, P., Jochum, K.P., 2012. OIB/seamount recycling as a possible process for E-MORB genesis. *Geochem., Geophys., Geosyst.* 13, QAAC19.
- Villalobos-Orchard, J., Freymuth, H., O'Driscoll, B., Elliott, T., Williams, H., Casalini, M., Willbold, M., 2020. Molybdenum isotope ratios in Izu arc basalts: the control of subduction zone fluids on compositional variations in arc volcanic systems. *Geochim. Cosmochim. Acta* 288, 68–82.
- Waters, C.L., Sims, K.W.W., Perfit, M.R., Blichert-Toft, J., Blusztajn, J., 2011. Perspective on the genesis of E-MORB from chemical and isotopic heterogeneity at 9–10°N East Pacific rise. *J. Petrol.* 52, 565–602.
- White, W.M., Dupré, B., 1986. Sediment subduction and magma genesis in the Lesser Antilles: isotopic and trace element constraints. *J. Geophys. Res.* 91, 5927–5941.
- Willbold, M., Elliott, T., 2023. Molybdenum isotope evidence for subduction-modified, recycled mafic oceanic crust in the mantle sources of ocean island basalts from La Palma and Hawaii. *Earth. Planet. Sci. Lett.* 621, 118399.
- Willbold, M., Hibbert, K., Lai, Y.-J., Freymuth, H., Hin, R.C., Coath, C., Vils, F., Elliott, T., 2016. High-precision mass-dependent molybdenum isotope variations in magmatic rocks determined by double-spike MC-ICP-MS. *Geostand. Geoanal. Res.* 40, 389–403.
- Wilson, S.C., Murton, B.J., Taylor, R.N., 2013. Mantle composition controls the development of an Oceanic Core Complex. *Geochem., Geophys., Geosyst.* 14, 979–995.
- Yang, S., Humayun, M., Salters, V.J.M., 2020. Elemental constraints on the amount of recycled crust in the generation of mid-oceanic ridge basalts (MORBs). *Sci. Adv.* 6, eaba2923.
- Zartman, R.E., Haines, S.M., 1988. The plumbotectonic model for Pb isotopic systematics among major terrestrial reservoirs - a case for bi-directional transport. *Geochim. Cosmochim. Acta* 52, 1327–1339.